Synergistic gold-bismuth Catalysis for Non-Mercury Hydrochlorination of Acetylene to Vinyl Chloride Monomer

Kai Zhou,[a] Wei Wang,[a] Zhun Zhao,[b] Guohua Luo,[a] Jeffrey T. Miller,[c] Michael S. Wong,[b,d,e] Fei Wei[a]

a. Beijing Key Laboratory of Green Reaction Engineering and Technology, Department of Chemical Engineering, Tsinghua University, Beijing 100084, China.

b. Dept. of Chemical and Biomolecular Engineering, Rice University, Houston, TX 77005-1892 USA.

c. Dept. of Chemical Science and Engineering, Argonne National Laboratory, Argonne, IL 60439, USA

d. Dept. of Chemistry, Rice University, Houston, TX 77005-1892 USA.

e. Dept. of Civil and Environmental Engineering, Rice University, Houston, TX 77005-1892 USA.

ABSTRACT: Gold has been proposed as an environmentally friendly catalyst for acetylene hydrochlorination for vinyl chloride monomer synthesis by replacing the commercially used mercury catalyst. However, long life with excellent activity of is difficult to achieve since gold is readily reduced to metallic nano-particles. The stability of gold limits its industrial application. In this paper, we promoted gold with bismuth for the hydrochlorination of acetylene. It was found that the Bi promotion leads to partial reduction to AuCl, rather than the complete reduction of Au to metallic nano-particles in the absence of Bi. The optimized catalyst with a molar ratio of Bi:Au=3:1 (0.3 wt% Au) showed comparable reactivity to 1.0 wt% Au catalyst and significantly improved stability. Furthermore, the gold-bismuth catalyst had higher activity and stability than the commercial mercury catalyst, is less toxic and more environmental-friendly, making it a potentially green mercury-free industrial catalyst for acetylene hydrochlorination.

Keywords: Gold catalysis; Hydrochlorination; Mercury-free; Synergistic catalysis; Au-Bi

Catalytic hydrochlorination of acetylene to vinyl chloride monomer (VCM) [Eq. (1)] by $HgCl_2$ is an important industrial process, which is facing increasing environmental pressure due to mercury pollution which occurs during commercial operation.

$$C_2H_2 + HCl \rightarrow CH_2CHCl \quad (1)$$

VCM is used in the production of polyvinyl chloride (PVC), an important plastic material. VCM is currently synthesized in Europe and the United States by the process of oxychlorination of ethylene obtained from petroleum. China is the largest producer of PVC, and approximately 80% of VCM production (15.86 $Mt \cdot a^{-1}$ production capacity) is obtained by acetylene hydrochlorination using C_2H_2, HCl and $HgCl_2$ catalyst.[1] This hydrochlorination route for PVC, which is derived from coal, has significant price advantage as long as the crude oil price is above about $80 per barrel. Because of the abundant coal reserve and historically high crude oil prices (> $100 p.b.) in China, the economically advantaged hydrochlorination process for production of PVC will likely continue in the foreseeable future.

Unfortunately, low heat transfer efficiency of industrial fixed bed reactors accompanied by the highly exothermic heat of reaction (ΔH= -124.8 $kJ \cdot mol^{-1}$)

leads to hot spots (>200 °C) and results in volatilization and loss of Hg from the catalyst. The $HgCl_2$ vapor released into the environment accumulates and causes chronic poisoning, which is harmful to humans and the environment. It is estimated that producing 1 ton of PVC requires 1.02-1.41 kg $HgCl_2$ catalyst with the mercury content ranging from 10 wt% to 15 wt%, and about 25% of the $HgCl_2$ fails to be reused during the recycling process in China.

Therefore, the development of a non-mercury hydrochlorination catalyst is a high priority. Gold, which was considered to be catalytically inert for a long-time, is now an attractive metal in catalysis since the discovery that small metallic Au nanoparticles were active for low-temperature CO oxidation and acetylene hydrochlorination.[2] Cationic gold, which is electrophilic and reactive with nucleophilic reactants, coordinates preferentially to alkene or alkyne making it possible to catalyze a variety of reactions ranging from partial oxidation of hydrocarbons, hydrogenation, and hydrodechlorination of unsaturated carbonyl and chlorinated compounds under various conditions.[3]

The Hutchings′ group[2b] has shown that the metal chlorides are catalytic for hydrochlorination and gold was the most active. Thereafter, highly efficient catalysts in the form of Au/C[2c, 2e, 4] demonstrate the feasibility of gold as a substitute for the toxic mercury catalyst. The potential for gold to catalyze acetylene hydrochlorination provides an alternative and environmentally friendly route for production of vinyl chloride monomer (VCM).

However, the present Au catalyst still faces significant obstacles for industrial applications, such as high cost and loading of Au, ca. 1.0 wt% [5] and rapid deactivation.[6] To overcome these disadvantages, several efforts have been made, such as adding Cu to the Au to promote the catalytic efficiency and decrease the Au loading to 0.5 wt%,[7] or co-feeding oxidizing gas like NO in an attempt to minimize the deactivation.[8] Although significant improvements have been achieved, further improvements are required in order to reduce the Au loading while maintaining stable catalytic performance.

Bismuth, a common non-precious metal, has been increasingly used as an environmental friendly element due to its low toxicity among heavy metals in recent years.[9] Wei et al. synthesized a bi-component Bi-Cu catalyst with 30% the activity of $HgCl_2$,[9] and demonstrated the catalyst in a 20 $t \cdot a^{-1}$ continuous fluidized bed reactor over 700 hrs. $BiCl_3$ is the active component and a steady-state conversion over 60% at 60 h^{-1} gas hourly space velocity (GHSV, acetylene based) was achieved during the test demonstrating the potential of this catalyst for industrial application.

In this paper, we described a novel hydrochlorination catalysts that employ $BiCl_3$ to promote Au in reactivity and stability. As shown in Fig. 1(a), the AuBi catalyst synthesized by impregnating Bi and Au on activated carbon (AC) simultaneously had higher catalytic efficiency and a lower deactivation rate compared to that reported for Au and AuCu catalysts (see Supporting Information for calculation methods). In addition, by modulating the mole ratio of Bi and Au to 3:1, it was possible to significantly reduce the Au loading (from 1.0 wt% down to 0.3 wt%) without loss in productivity. Compared to the conventional 9.0 wt% Hg/C and 1.0 wt% Au/C, the optimized AuBi catalyst had enhanced reactivity as shown in Fig. 1(b). The beneficial role of Bi for Au is largely unknown; however, and it was speculated that there was significant electron transfer from Bi to Au contributing to the enhancement of C_2H_2 absorption. Alternatively, Bi was thought to significantly enhance the dispersion of Au nano-particles, stabilize Au in the state of Au^+ and leading to higher activity.

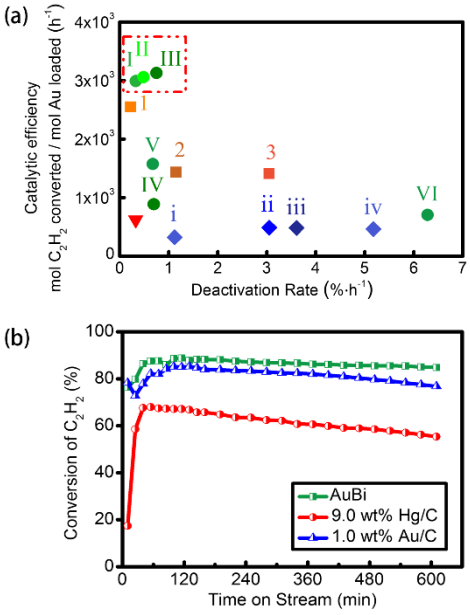

Figure 1. (a) The comparison of catalytic efficiency and the deactivation rate of 3 series catalysts: ● (green color): **I.** 0.3 wt% AuBi (Bi:Au=3:1), **II.** 0.3 wt% AuBi (Bi:Au=5:1), **III.** 0.3 wt% AuBi (Bi:Au=20:1), **IV.** 1.0 wt% Au, **V.** 0.5 wt% Au/C, **VI.** 0.3 wt% Au/C. ♦ (blue color): **i.** 1.0 wt% Au/C, **ii.** AuRh (Au:Rh=50:50), **iii.** AuIr (Au:Ir=99:1), **iv.** AuPd (Au:Pd=99:1).[10] ■ (orange color):

1. 0.5 wt% AuCu (Au:Cu=1:5), **2.** 1.0 wt% Au/C, **3.** 0.5 wt% Au/C.[11]▼ (red color): Au(1.0 wt%).[5b] (T=180 °C, GHSV(C_2H_2)=600 h^{-1}) (b) The comparison of the reactivity and stability of 3 catalysts: 0.3 wt% AuBi (Bi:Au=3:1), 9.0 wt% Hg/C and 1.0 wt% Au/C. (All ratios were based on molar ratio, T=180 °C, GHSV(C_2H_2)=600 h^{-1})

Generally, catalytic activity was correlated with Au content and the number of active sites for the adsorption of HCl and C_2H_2 i.e., the dispersion of Au. To verify this relationship for Au, 3 catalysts containing 1.0 wt%, 0.5 wt% and 0.3 wt% Au were evaluated at 600 h^{-1} of GHSV and 180 °C. As shown in Fig. 2(a), the conversion decreased from 80% to less than 20% when Au content decreased from 1.0 wt% to 0.3 wt%. High conversions required high Au loading.

Introducing Bi into the catalyst significantly increased the activity compared to mono-component Au. As shown in Fig. 2(b), catalyst AuBi (0.3 wt%, Bi:Au=3:1, mole ratio; *i.e.* 0.3 wt% Au and 0.95 wt% Bi) had over 3 times the conversion over the algebraic sum of 0.3 wt% Au/C and 0.95 wt% Bi/C catalysts. The promotion of Au by small amounts of $BiCl_3$ significantly improved the conversion and stability (better than the 1.0 wt% Au/C), and reduced the Au loading by 2/3. The higher activity of the bi-component catalyst suggested there was an interaction between active metals not present in the mono-component catalysts.

In order to determine the optimized ratio of Au and Bi, the ratio of Bi:Au was varied from 1 to 20 as shown in Fig. 2(c). As the ratio of Bi:Au increased from 1 to 3, the conversion increased rapidly; as the ratio was further increased, there was little increase in the conversion. Based on these results, a Bi:Au ratio 3 was considered optimized, and 'AuBi' was specified for the optimized formula.

To understand the role of Bi on Au, the bi-component and mono-component Au catalysts were characterized. Fig. S1(a), S1(c) and S2 show the SEM and TEM images of as-prepared Au catalysts. 0.3 wt% Au/C had numerous Au particles of various sizes on the AC. The diameters generally were larger than 20 nm with some over 100 nm. ~~Fig. S1(b) and S1(d)~~TEM and SEM images shows that adding $BiCl_3$ significantly improved the dispersion of Au with fewer large particles and most of existed nanoparticles were less than about 5 nm in diameter. XRD patterns in Fig. 3(c) are also consistent with this conclusion, where 0.3 wt% Au/C had strong diffraction peaks of Au indicating the presence of large crystals (d_{mean}=28 nm according to Scherrer formula), while AuBi had no characteristic peaks of metallic Au nano-particles, suggesting good dispersion of Au on the AC.

Figure 2. (a) The catalytic performance of Au/C with different Au loading content: 0.3 wt%, 0.5wt% and 1.0 wt%. (b) The catalytic performance of 0.3 wt% Au/C, 0.3wt% Bi/C and AuBi in which the gold content was 0.3 wt%. (c) The catalytic performance of 0.3wt% AuBi with different Bi mole ratio, Bi:Au=1:1, 3:1, 5:1 and 20:1. The evaluation conditions: T=180 °C, Q(C_2H_2):Q(HCl)=1.0:1.1, GHSV=600 h^{-1}.

To further understand if there was also a chemical effect of Bi on the structure of Au, 3 synthesis routes of AuBi series catalysts were investigated. As shown in Fig. 3(a), catalyst named as AuBi was synthesized via route 1 by co-impregnation of an aqueous solution of $HAuCl_4$ and $BiCl_3$ onto AC. Synthesis route 2, catalyst abbreviated as AuBi-I, was made through by first impregnating Au^{3+} (aq) on AC followed by impregnating Bi^{3+} (aq) on Au/C after drying. Preparation 3, catalyst AuBi-II, was similar to route 2 but the impregnation order of $HAuCl_4$ and $BiCl_3$ was reversed. All three catalysts contained 0.3 wt% Au and 0.95 wt% Bi with a Bi:Au mole ratio of 3:1. Fig. 3(b) shows the activity of three catalysts: AuBi and AuBi-I had similar and stable conversion during the 10 hrs' test. The activity of AuBi-II was relatively poor and unstable, even lower than the algebraic sum conversion of 0.3 wt% Au/C and 0.95 wt% Bi/C. XRD patterns in Fig. 3(c) showed that no Au peaks

in AuBi existed, indicating Au or Bi related nano-crystals were not well formed. Different from AuBi, AuBi-I had weak but visible diffraction peaks of Au, while AuBi-II and 0.3 wt% Au/C had strong and sharp peaks. AuBi had stable conversion without significant Au nano-particle formation after 10 hrs' test (See XRD patterns in Fig. S3), revealing the valuable improvement of Au dispersion after the introduction of Bi in AuBi.

The different catalytic behaviors among these 3 catalysts were in accordance with the role of Bi. The Bi compounds generally had low solubility in water; therefore the impregnation of $BiCl_3$ at first step induced $BiCl_3$' precipitation from solution, which hindered the dispersion of and the interaction with Au cations. Differently, precipitated $AuCl_3$ in the fresh Au/C could partially re-dissolve and the 2 cations interacted with each other during the impregnation of $BiCl_3$, and very tiny particles was formed promoted by Bi^{3+}. Generally, the high dispersion of metals increased the amount of active sites. According to the analysis of SEM, TEM, XRD and reactivity, the high hydrochlorination rate of the AuBi catalysts likely resulted from the much higher Au dispersion.

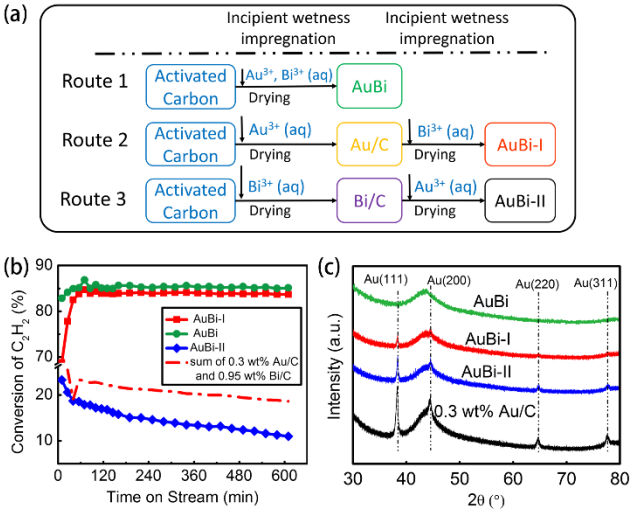

Figure 3. (a) The schematic diagram of 3 different routes to synthesize AuBi catalyst. (b) Catalytic performance of catalysts prepared by the single-step method and two-step method. Reaction conditions: T=180 °C, GHSV(C_2H_2)=600 h^{-1}. (c) XRD patterns of 0.3 wt% Au/C, AuBi, AuBi-I and AuBi-II.

XRD patterns proved that no significant metallic Au crystals were formed in AuBi, however, the chemical valence state of Au needed further investigation. Temperature programmed reduction (TPR) analysis of the bi-component AuBi and mono-component catalysts (0.95 wt% Bi/C and 0.3 wt% Au/C) were obtained in order to determine differences in reducibility. As shown in Fig. 4(a), the maximum H_2 consumption peaks of 0.95 wt% Bi/C and 0.3 wt% Au/C appeared at 450 °C and 353 °C respectively without any visible overlapped peaks, thought to be the reduction of Bi^{3+} and Au^{3+} species. The peaks in the AuBi was decomposed into 2 peaks with temperature at 425 °C and 332 °C respectively, between that of Bi/C and Au/C, identified to be the Bi^{3+} and single species of Au cations. The temperature shift of the maximum consumption to lower temperature (over 20 °C) was thought to be the sign of interaction between Au and Bi.

X-ray photoelectron spectra (XPS) was used to further verify the valence states evolution of the bi-component catalyst. Fig. 4(b) showed the XPS region spectra of Bi4f in the Bi/C and AuBi. $Bi4f_{7/2}$ and $Bi4f_{5/2}$ peaks corresponding to the Bi^{3+} were located at 159.9 and 165.2 eV, respectively, assigned to $BiCl_3$.[12] The peaks attributed to the metallic state of Bi (at 156.4 and 161.6 eV) weren't present in the sample, indicating that in Bi/C that active site was Bi^{3+} species, present as $BiCl_3$. The similar Bi4f signals were observed in the AuBi, the binding energy of Bi peaks were slightly lower, 159.4 and 164.7 eV, than that in Bi/C. The shift to lower binding energy was attributed the presence of smaller nanoparticles of $BiCl_3$, suggesting the improvement of Bi dispersion into tiny particles. The Au XPS spectrum of Au/C and AuBi were shown in Fig. 4(c). The detailed fitting analysis indicated that for each oxidation state of Au there had two peaks separated by *ca.* 3.7 eV, corresponding to $4f_{7/2}$ (lower binding energy) and $4f_{5/2}$ (higher binding energy) spin orbit states. Using the known electron binding energies for the various oxidation states of Au, [13] the $4f_{7/2}$ peaks at 84.0, 85.1, and 86.8 eV were assigned as Au^0, Au^+ and Au^{3+}, respectively. The $4f_{5/2}$ peaks at 87.7, 88.4, and 90.5 eV are due to Au^0, Au^+ and Au^{3+}, respectively.[2e, 14] 32% Au^0 and 68% Au^{3+} existed in the Au/C, which coincided well with the previous publications.[2e, 8] The surprising results was that the valence state of Au was 100% pure Au^+ in the AuBi, which was quite different from that of Au/C. Generally, individual Au^+ was thought to be unstable during the reaction due to its higher reduction potential (1.15 V). However, we discovered the enhancement in stability of Au^+ in the catalyst after intro-

duction of Bi. The strong stability facilitates its good performance in hydrochlorination thereafter.

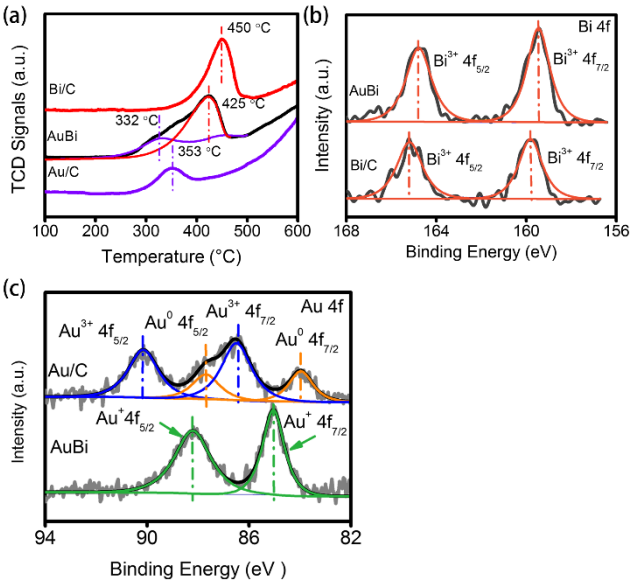

Figure 4. (a) TPR analysis of 0.95 wt% Bi/C, 0.3 wt% Au/C and AuBi; (b) Bi 4f XPS spectra in Bi/C and AuBi, $Bi4f_{7/2}$ and $Bi4f_{5/2}$ peaks corresponding to the Bi^{3+} were located at 159.9 and 165.2 eV, respectively, assigning to $BiCl_3$; (c). Au 4f XPS spectra in Au/C and AuBi. The peaks at 84.0, 85.1 and 86.8 eV were the $4f_{7/2}$ peak of Au^o, Au^+ and Au^{3+}, respectively; the peaks at 87.7, 88.4 and 90.5 eV were the $4f_{5/2}$ peak of Au^o, Au^+ and Au^{3+}.

To further investigate the precise formal valence, coordination environment and subtle geometrical distortions of Au and Bi in AuBi catalyst, X-ray absorption spectroscopy (XAS) was employed. X-ray absorption near edge structure (XANES) energy, which is the inflection point of the leading edge, is dependent on both the oxidation state of detected elements and the types of ligands. Fig. S4 shows the XANES data of standard Au species, which are Au^o, Au^+ and Au^{3+}. The spectra indicated the XANES energy of Au^o and Au^+ were similar, but Au^{3+} was at lower energy. These references compounds were used to fit the unknown samples do determine the fractional composition of oxidation states.

The fresh and spent (reaction over 600 min) AuBi was analyzed by XANES and EXAFS (Extended x-ray absorption fine structure) both under air at room temperature and under He at room temperature after being treated with H_2 flow at 200 °C (Supporting Information), which was shown in Fig. 5. Both the XANES and EXAFS spectra of Au edge were consistent with Au-Cl coordination with no indication of metallic Au NP's in either sample, indicating the Au species was AuCl. XANES fitting (100% Au^+, Table S1) and EXAFS fitting (~2.0 coordination number for Au-Cl scatter, Table S1) were consistent AuCl in all catalysts. The XANES and EXAFS of Bi in fresh and spent samples were identical, and were consistent with Bi^{3+}, indicating there were no metallic Bi bonds (Fig. 5(b) and (d)). The magnitude of FT, which was proportional to the number of bonds was within the error the same in all catalysts. The fitting of EXAFS spectra at Bi edge was consistent with three Bi-Cl bonds (~3.0 coordination number for Bi-Cl scatter, Table S1), and the Bi-Cl distance was 2.50 Å in air, the same as in the $BiCl_3$ reference. After reduction at 200 °C, the Bi-Cl bonds were slightly shorter, *ca.* 2.47 Å. At Au edge, there was no evidence of any Au-Bi bond in any catalyst. At Bi edge, there was also no evidence of any Bi-Au bond in any catalyst.

For both fresh and spent catalyst, it was unusual that Au was not reduced to metallic nano-particles' under H_2 at 180°C (Table S1). Taking into account that there was no apparent chemical bonding between Au and Bi, it was clear that Bi chloride inhibited the reduction of Au cations to metallic Au, and only AuCl was formed.

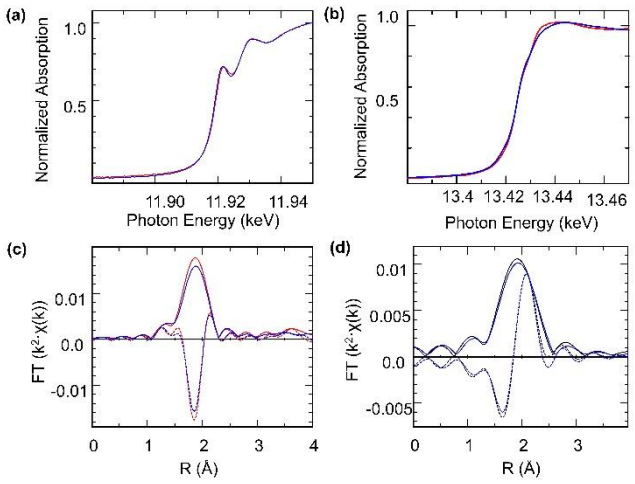

Figure 5. (a) Au L_3 XANES from 11.98 to 11.95 keV for AuBi in air and H_2 at 200 °C; (b) Bi L_3 XANES from 13.37 to 13.47 keV for AuBi in air and H_2 at 200 °C; (c) Au L_3Fourier transform of the EXAFS for AuBi in air and H_2 at 200 °C (k^2: Δk = 2.9 – 11.8 Å; solid-magnitude FT and dotted-imaginary part FT); (d) Au L_3 Fourier transform of the EXAFS for AuBi in air and H_2 at 200 °C (k^2: Δk = 2.7 – 8.7 Å; solid-magnitude FT and dotted-imaginary part FT). (Red: AuBi in air at room

temperature, Blue: AuBi in H_2 at 200 °C, Black: $BiCl_3$ Standard).

The interesting catalytic performance of bi-component catalyst is speculated from the introduction of Bi^{3+}. Bi^{3+}, which has good dispersion, promotes the Au cations in the form of tiny particles and separates those active microcrystals from sintering and growing up. As a result, the bi-component catalyst can maintain high activity and stability for a long time. The stable presence of Au^{+} rather than Au^{3+} may be attributed to some weak interaction between Bi^{3+} and Au species. Generally, fresh Au catalyst has both Au^{3+} and Au^{0} species due to partial reduction of Au^{3+} in solution and air. Bi^{3+}, performing as an electron transfer on the other hand, transfers electrons between Au^{3+} and Au^{0}, and stabilizes Au in state of Au^{+} either in preparation or reaction. The tiny blue shift of XPS spectrum of Bi suggests some co-effect between Au^{+} and Bi^{3+}. However, more detailed understanding needs studying by theoretical chemistry.

The catalytic performance of a range of carbon-supported platinum group metals for the hydrochlorination of C_2H_2 was investigated by Hutchings, [2b, 8, 15] and the experimental data showed a linear correlation of the performance with the standard electrode potential by correlating the initial activity of the catalyst with the standard electrode potential of the metals. Because the introduction of Bi didn't change the structure of AuCl, the turnover frequency (TOF) of AuBi was calculated to compare with the previous published results. As Fig. 6(a) shown, the Au nanoparticles had a mean diameter of 6.1±1.7 nm (counting over 200 particles) by TEM. With an electrode potential for Au^{+} of 1.15 V, the TOF, which was 184 min^{-1} (Table S2), was in good agreement with the linear relationship as Fig. 6(b) shown (the calculation procedure followed Hutchings group' method).[2c] Although the effect of Bi in activity shouldn't be ignored, the rate of $BiCl_3$ was relatively poor. The main role of Bi in promoting gold's activity is to stabilize the formation of AuCl, which has enhanced hydrochlorination TOF. Bismuth's ability to suppress reduction of Au to metallic nanoparticles is the reason for excellent stability.

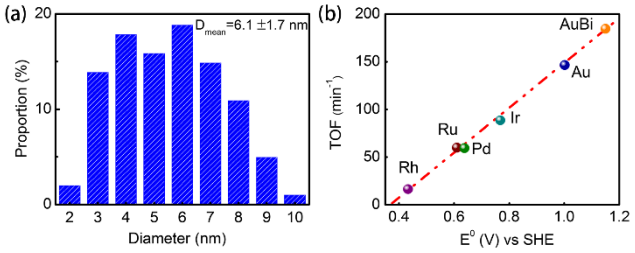

Figure 6. (a) The statistics of the particles' diameter in catalyst AuBi;* (b) Correlation between TOF values versus the standard electrode potential of AuBi and other various metals[15]. Potentials are obtained from the reduction potentials of the following chloride salts $(RhCl_6)^{3-}$, $(RuCl_5)^{2-}$, $PdCl_2$, $(PtCl_6)^{2-}$, $(IrCl_6)^{3-}$, $(AuCl_4)^{-}$ and AuCl in AuBi to the corresponding metals. (*See more information about particles' diameter calculations in SI)

Overall, the synergistic effect between Bi and Au led to a reduction in the Au loading to about 0.3 wt%. In addition, Bi stabilized the Au^{+} by inhibiting the reduction to metallic Au. In the absence of Bi, Au nano-particles with a diameter of 28 nm were formed, which have significantly lower activity and stability. The ultralow-Au bi-component catalyst had superior activity (TOF=184 min^{-1}) and stability than the conventional mercury catalyst, was less toxic and more environmental-friendly. Thus, AuBi shows great promise as a green, mercury-free industrial hydrochlorination catalyst.

ASSOCIATED CONTENT

Experimental details were supplied in the supporting information. This material is available free of charge via the Internet at http://pubs.acs.org.

AUTHOR INFORMATION

Corresponding Author:

luoguoh@tsinghua.edu.cn (Guohua Luo);

wf-dce@tsinghua.edu.cn (Fei Wei)

Notes: The authors declare no competing financial interests.

ACKNOWLEDGMENT

Financial support from the Ministry of Science and Technology of China (projects: 2008BAB41B02, 2012AA062901) is highly appreciated. Support from the National Science Foundation (CBET-1134535) is also gratefully acknowledged (MSW). JTM was supported by the U.S. Department of Energy, Office of Basic Energy Sciences, Chemical Sciences under Contract DE-AC-02-06CH11357. The use of the Advanced Photon Source

(APS) was supported by the U. S. Department of Energy, Office of Science, Office of Basic Energy Sciences, under Contract No. DE-AC02-06CH11357. Materials Research Collaborative Access Team operations are supported by the Department of Energy and the MRCAT member institutions.

REFERENCES

1. Bing, J.; Li, C. *Polyvinyl Chloride* **2011,** *39*, 1-8.

2. (a) Haruta, M.; Kobayashi, T.; Sano, H.; Yamada, N. *Chem. Lett.* **1987,** *2*, 405-408. (b) Hutchings, G. J. *J. Catal.* **1985,** *96*, 292-295. (c) Conte, M.; Davies, C. J.; Morgan, D. J.; Davies, T. E.; Elias, D. J.; Carley, A. F.; Johnston, P.; Hutchings, G. J. *J. Catal.* **2013,** *297*, 128-136. (d) Finch, R. M.; Hodge, N. A.; Hutchings, G. J.; Meagher, A.; Pankhurst, Q. A.; Siddiqui, M. R. H.; Wagner, F. E.; Whyman, R. *Phys. Chem. Chem. Phys.* **1999,** *1*, 485-489. (e) Conte, M.; Davies, C. J.; Morgan, D. J.; Davies, T. E.; Carley, A. F.; Johnston, P.; Hutchings, G. J. *Catal. Sci. Technol.* **2013,** *3*, 128-134.

3. (a) Zhang, X.; Shi, H.; Xu, B. Q. *J. Catal.* **2011,** *279*, 75-87. (b) Hashmi, A. S. K.; Hutchings, G. J. *Angew. Chem. Int. Edit.* **2006,** *45*, 7896-7936. (c) Hashmi, A. S. K.; Buehrle, M. *Aldrichim. Acta.* **2010,** *43*, 27-33. (d) Marco, C.; Graham, H. *Modern Gold Catalyzed Synthesis*. Wiley-VCH Verlag GmbH & Co. KGaA: 2012. (e) A. Stephen K., H.; Miriam, B. *Aldrichim. Acta.* **2010,** *43*, 27-33. (f) Wei, Y.; Liu, J.; Zhao, Z.; Chen, Y.; Xu, C.; Duan, A.; Jiang, G.; He, H. *Angew. Chem. Int. Edit.* **2011,** *50*, 2326-2329. (g) Xue, W. J.; Wang, Y. F.; Li, P.; Liu, Z.-T.; Hao, Z. P.; Ma, C. Y. *Catal. Comm.* **2011,** *12*, 1265-1268. (h) Gaudet, J.; Bando, K. K.; Song, Z.; Fujitani, T.; Zhang, W.; Su, D. S.; Oyama, S. T. *J. Catal.* **2011,** *280*, 40-49. (i) Date, M.; Okumura, M.; Tsubota, S.; Haruta, M. *Angew. Chem. Int. Edit.* **2004,** *43*, 2129-2132. (j) Budroni, G.; Kondrat, S. A.; Taylor, S. H.; Morgan, D. J.; Carley, A. F.; Williams, P. B.; Hutchings, G. J. *Catal. Sci. Technol.* **2013,** *3*, 2746-2754. (k) Zhang, X.; Corma, A. *Angew. Chem. Int. Edit.* **2008,** *47*, 4358-4361. (l) Krauter, C. M.; Hashmi, A. S. K.; Pernpointner, M., *Chemcatchem* **2010,** *2* (10), 1226-1230. (m) Lein, M.; Rudolph, M.; Hashmi, S. K.; Schwerdtfeger, P., *Organometallics* **2010,** *29* (10), 2206-2210.

4. (a) Hutchings, G. J.; Joffe, R. *Appl. Catal.* **1986,** *20*, 215-218. (b) Hutchings, G. J. *Catal. Today* **2002,** *72*, 11-17. (c) Hutchings, G. J. *Top. Catal.* **2008,** *48*, 55-59.

5. (a) Zhang, H.; Dai, B.; Wang, X.; Li, W.; Han, Y.; Gu, J.; Zhang, J. *Green Chem.* **2013,** *15,* 829-836. (b) Zhang, H.; Dai, B.; Wang, X.; Xu, L.; Zhu, M. *J. Ind. Eng. Chem.* **2012,** *18*, 49-54.

6. Zhang, J.; He, Z.; Li, W.; Han, Y. *Rsc Adv.* **2012,** *2*, 4814-4821.

7. Wang, S. J.; Shen, B. X.; Song, Q. L. *Catal. Lett.* **2010,** *134*, 102-109.

8. Nkosi, B.; Adams, M. D.; Coville, N. J.; Hutchings, G. J. *J. Catal.* **1991,** *128*, 378-386.

9. (a) Wei, X. B.; Wei, F.; Qian, W. Z.; Luo, G. H.; Shi, H. B.; Jin, Y. *Chin. J. Process Eng.*, **2008,** 8, 1218-1222. (b) Zhou, K.; Jia, J.; Li, X.; Pang, X.; Li, C.; Zhou, J.; Luo, G.; Wei, F. *Fuel Process. Technol.* **2013,** *108*, 12-18.

10. Conte, M.; Carley, A. F.; Attard, G.; Herzing, A. A.; Kiely, C. J.; Hutchings, G. J. *J. Catal.* **2008,** *257*, 190-198.

11. Wang, S.; Shen, B.; Song, Q. *Catal. Lett.* **2010,** *134*, 102-109.

12. (a) Ling, B.; Sun, X. W.; Zhao, J. L.; Shen, Y. Q.; Dong, Z. L.; Sun, L. D.; Li, S. F.; Zhang, S. *J. Nanosci. Nanotechno.* **2010,** *10*, 8322-8327. (b) Zhao, X.; Ren, M.; Bruns, M.; Fichtner, M. *J. Power Sources* **2014,** 245, 706–711.

13. (a) Ozkaraoglu, E.; Tunc, I.; Suzer, S. *Surf. Coat. Technol.* **2007,** *201*, 8202-8204. (b) Ozkaraoglu, E.; Tunc, K.; Suzer, S. *Polymer* **2009,** *50*, 462-466.

14. Fong, Y.-Y.; Visser, B. R.; Gascooke, J. R.; Cowie, B. C. C.; Thomsen, L.; Metha, G. F.; Buntine, M. A.; Harris, H. H. *Langmuir* **2011,** *27*, 8099-8104.

15. (a) Nkosi, B.; Coville, N. J.; Hutchings, G. J. *J. Chem. Soc., Chem. Commun.* **1988,** 1, 71-72. (b) Nkosi, B.; Coville, N. J.; Hutchings, G. J. *Appl. Catal.* **1988,** *43*, 33-39. (c) Conte, M.; Carley, A. F.; Heirene, C.; Willock, D. J.; Johnston, P.; Herzing, A. A.; Kiely, C. J.; Hutchings, G. J. *J. Catal.* **2007,** *250*, 231-239.

Insert Table of Contents artwork here